The Plant Journal (2004) **37**, 839–852 doi: 10.1111/j.1365-313X.2003.02011.x

Mutants for photosystem I subunit D of *Arabidopsis thaliana*: effects on photosynthesis, photosystem I stability and expression of nuclear genes for chloroplast functions

Anna Ihnatowicz[1], Paolo Pesaresi[1], Claudio Varotto[2], Erik Richly[1], Anja Schneider[3], Peter Jahns[4], Francesco Salamini[1] and Dario Leister[1,*]

[1]*Abteilung für Pflanzenzüchtung und Ertragsphysiologie, Max-Planck-Institut für Züchtungsforschung, Carl-von-Linné Weg 10, D-50829 Köln, Germany,*

[2]*Zentrum zur Identifikation von Genfunktionen durch Insertionsmutagenese bei Arabidopsis thaliana (ZIGIA), Max-Planck-Institut für Züchtungsforschung, Carl-von-Linné Weg 10, D-50829 Köln, Germany,*

[3]*Botanisches Institut der Universität zu Köln, Gyrhofstrasse 15, D-50931 Köln, Germany, and*

[4]*Institut für Biochemie der Pflanzen, Heinrich-Heine-Universität Düsseldorf, Universitätsstraße 1, 40225 Düsseldorf, Germany*

Received 8 October 2003; revised 28 November 2003; accepted 9 December 2003.
*For correspondence (fax +49 221 5062413; e-mail leister@mpiz-koeln.mpg.de).

Summary

In *Arabidopsis thaliana*, the D-subunit of photosystem I (PSI-D) is encoded by two functional genes, *PsaD1* and *PsaD2*, which are highly homologous. Knock-out alleles for each of the loci have been identified by a combination of forward and reverse genetics. The double mutant *psad1-1 psad2-1* is seedling-lethal, high-chlorophyll-fluorescent and deficient for all tested PSI subunits, indicating that PSI-D is essential for photosynthesis. In addition, *psad1-1 psad2-1* plants show a defect in the accumulation of thylakoid multiprotein complexes other than PSI. Of the single-gene mutations, *psad2* plants behave like wild-type (WT) plants, whereas *psad1-1* markedly affects the accumulation of *PsaD* mRNA and protein, and photosynthetic electron flow. Additional effects of the *psad1-1* mutation include a decrease in growth rate under greenhouse conditions and downregulation of the mRNA expression of most genes involved in the light phase of photosynthesis. In the same mutant, a marked decrease in the levels of PSI and PSII polypeptides is evident, as well as a light-green leaf coloration and increased photosensitivity. Increased dosage of *PsaD2* in the *psad1-1* background restores the WT phenotype, indicating that PSI-D1 and PSI-D2 have redundant functions.

Keywords: *Arabidopsis thaliana*, expression profile, mutant, photosynthesis, photosystem I, PSI-D.

Introduction

Photosystem I (PSI) mediates light-driven electron transport across the thylakoid membrane. The PSI complexes of cyanobacteria and plants are functionally and structurally similar, and the crystal structure of cyanobacterial PSI has recently been established (Jordan *et al.*, 2001). Plant PSI is slightly larger than its cyanobacterial pendant (Kitmitto *et al.*, 1997), and trimer formation has been observed only in cyanobacteria (Chitnis and Chitnis, 1993). In plants, the PSI core is associated with the light-harvesting complex I (LHCI), which consists of four different pigment-binding polypeptides (Jansson, 1999). In addition, of the 14 polypeptides that form the core of PSI in flowering plants (PSI-A to -L and PSI-N to -O; Knoetzel *et al.*, 2002; Scheller *et al.*, 2001), four (G, H, N and O) have no counterpart in cyanobacteria. Conversely, no homologue of the cyanobacterial PSI-M has yet been discovered in flowering plants.

The three subunits PSI-A, -B and -C, which bind the electron acceptors, are crucial for PSI function. In *Arabidopsis*, these proteins, together with PSI-I and -J, are encoded by plastid DNA, whereas all other subunits are encoded by the nuclear genome. Two gene copies each for PSI-D, -E and -H exist. Downregulation of individual PSI subunits by antisense or co-suppression strategies, combined with the identification of insertion mutants, has provided the basis for the functional analysis of almost all nucleus-encoded PSI polypeptides (Haldrup *et al.*,

1999, 2000; Jensen *et al.*, 2000, 2002; Lunde *et al.*, 2000; Naver *et al.*, 1999; Varotto *et al.*, 2000a, 2002a).

Ferredoxin – and in cyanobacteria and some algae, also flavodoxin – is reduced at the stromal face of PSI by the extrinsic subunits C, D and E. These three polypeptides form a compact interconnected structure, the so-called stromal ridge (Jordan *et al.*, 2001; Klukas *et al.*, 1999; Kruip *et al.*, 1997). In cyanobacteria, loss-of-function mutants for each of the corresponding genes have been characterized. PSI-C is necessary for the stable association of PSI-D, -E and -L (Mannan *et al.*, 1994; Yu *et al.*, 1995). Cells that lack PSI-D are affected in photoautotrophic growth and in flavodoxin-mediated photoreduction of $NADP^+$, and moreover, they show no ferredoxin-mediated $NADP^+$ photoreduction at all (Chitnis *et al.*, 1989; Xu *et al.*, 1994). Lines in which PSI-E is missing are impaired in $NADP^+$ photoreduction, but exhibit normal photoautotrophic growth (Xu *et al.*, 1994; Zhao *et al.*, 1993).

The eukaryotic PSI-D and -E subunits are larger than their cyanobacterial counterparts, containing N-terminal extensions of 25–30 amino acids. In the *psae1-1* mutant of *Arabidopsis thaliana*, knocked-out for one of the two genes coding for PSI-E, the level of PSI-E and concomitantly those of PSI-C and -D, are significantly reduced. The oxidation state of PSI, photosynthetic state transitions and photoautotrophic growth are also altered in this mutant (Pesaresi *et al.*, 2002; Varotto *et al.*, 2000a).

Recently, the analysis of antisense lines with 5–60% of PSI-D showed that downregulation of PSI-D de-stabilizes PSI, results in increased photosensitivity and in an altered thiol disulphide redox state of the stroma (Haldrup *et al.*, 2003). Here, we characterize the effects of complete lack of PSI-D, as well as the impact of the two *PsaD* genes on PSI-D function. Disruption of the *PsaD1* gene, but not of *PsaD2*, affects the composition of PSI, alters the redox state of the photosynthetic apparatus, and impairs plant growth in the greenhouse. Analysis of the expression of nuclear genes for chloroplast proteins reveals further physiological effects of the *psad1-1* mutation. Overexpression analysis indicates that the products of the two *PsaD* genes have redundant functions. The absence of both functional *PsaD* genes is incompatible with the accumulation of functional PSI, affects the accumulation of all other thylakoid multiprotein complexes and is lethal at the seedling stage.

Results

Identification and phenotype of PSI-D mutants

Screening of a collection of *Arabidopsis* lines carrying independent insertions of the *dSpm* transposon (the Sainsbury Laboratory Arabidopsis Transposants (SLAT) collection; Tissier *et al.*, 1999) for alterations in the effective quantum yield of PSII (Φ_{II}; Varotto *et al.*, 2000b) resulted in the identification of the mutant line *photosynthesis-affected mutant 62* (*pam62*). The photosynthetic lesion was inherited as a recessive trait, and RFLP analysis of plants segregating for the *pam62* mutation with a *dSpm*-specific probe revealed the presence of only one transposon copy that co-segregated with the mutant allele (data not shown). Isolation of genomic sequences flanking the termini of the *dSpm* insertion was achieved by inverse PCR as described by Tissier *et al.* (1999), and the insertion site was identified. The *dSpm* transposon was inserted in the unique exon of the *PsaD1* gene (At4g02770) coding for PSI-D (Figure 1a), and the mutant *pam62* was accordingly designated *psad1-1*.

In the *A. thaliana* genome, a second *PsaD* gene (*PsaD2,* At1g03130) exists, which codes for a protein highly homologous to the *PsaD1* gene product (96/95% similarity/identity; Figure 2). After cleavage of predicted chloroplast transit peptides (domain I in Figure 2), the proteins PSI-D1 and -D2 differ only in the highly variable plant-specific N-terminal extension (domain II). To establish the photosynthetic function of *PsaD2*, the database SIGNAL (http://signal.salk.edu/cgi-bin/tdnaexpress; Alonso *et al.*, 2003) was

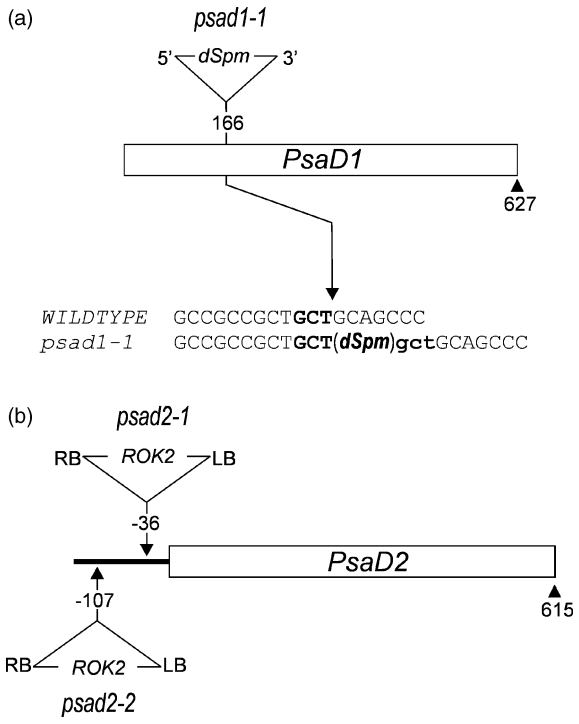

Figure 1. Tagging of the *PsaD1* and *PsaD2* genes.
(a) In *psad1-1*, the *PsaD1* gene (At4g02770) is disrupted by an insertion of the non-autonomous *dSpm* element (Tissier *et al.*, 1999). Upper case letters indicate plant DNA sequences flanking the *dSpm* element, bold uppercase letters indicate the transposon target site in WT and the duplicated target site is indicated by bold lowercase letters.
(b) The *psad2-1* and *psad2-2* mutants carry insertions of the 5.2-kbp pROK2 T-DNA (http://www.signal.salk.edu) in the promoter region of the *PsaD2* gene (At1g03130).The *dSpm* and T-DNA insertions are not drawn to scale.

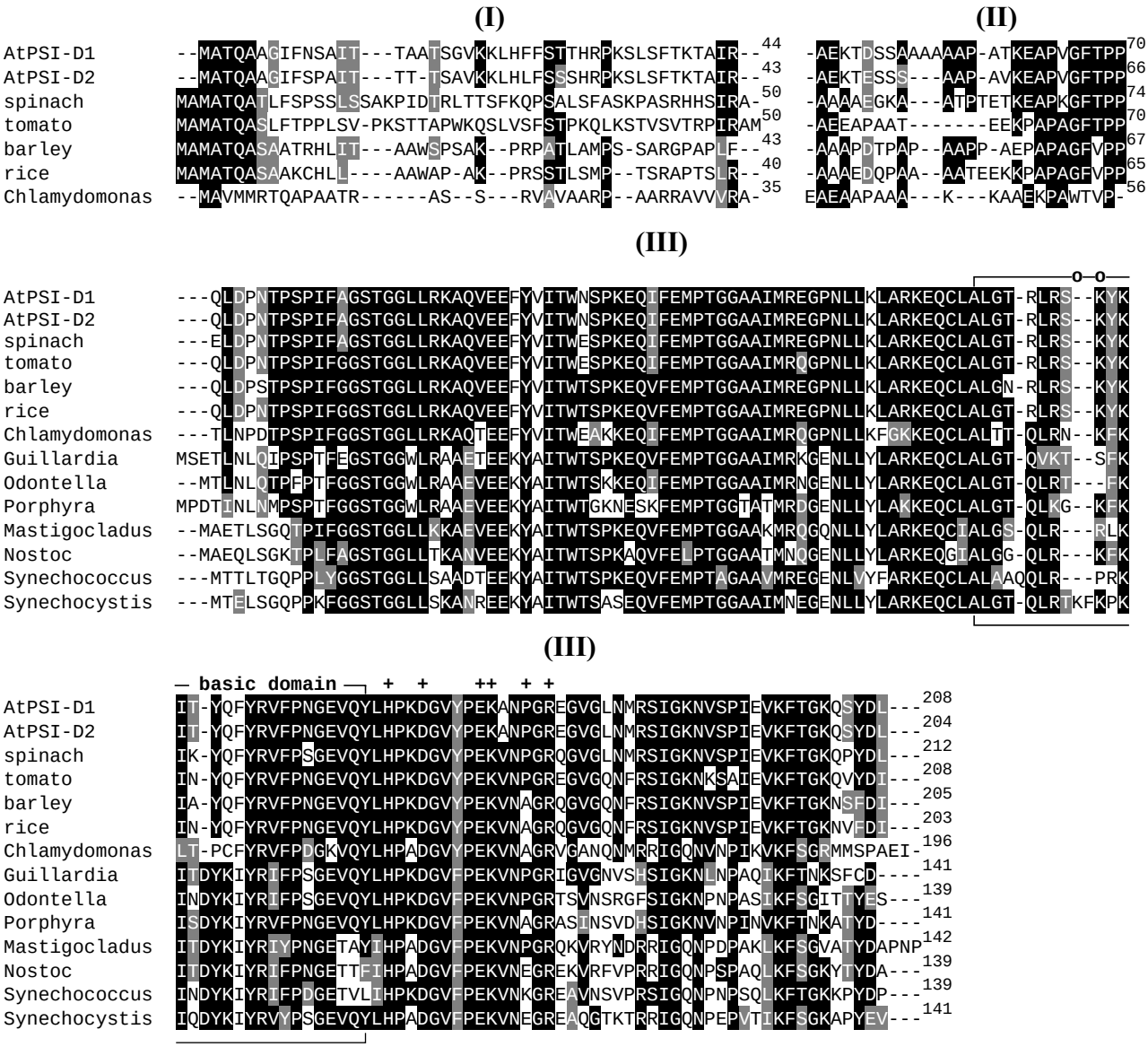

Figure 2. Comparison of PSI-D protein sequences from higher plants, algae and prokaryotes.
The amino acid sequences of the *Arabidopsis* PSI-D1 and -D2 proteins (Accession numbers: At4g02770 and At1g03130) were compared with those of PSI-D from spinach (GI:19855891), tomato (GI:82100), barley (GI:478404), rice (GI:29367391) and with PSI-D sequences from the green alga *Chlamydomonas reinhardtii* (GI:498824), the red alga *Porphyra purpurea* (GI:2147918), the cryptophyte alga *Guillardia theta* (GI:3603032), the chlorophyll *a*/*c* containing alga *Odontella sinensis* (GI:7443141) and from four cyanobacterial species: *Nostoc* sp. PCC 8009 (GI:5052771), *Synechocystis* sp. PCC 6803 (GI:16329280), *Synechococcus* sp. (GI:47576) and *Mastigocladus laminosus* PCC 7605 (GI:2160762). The three-part alignment shows the N-terminal chloroplast transit peptide of higher plant and *Chlamydomonas* PSI-D (I), which was either experimentally determined (spinach, tomato, barley, *Chlamydomonas*) or predicted by TARGETP (*Arabidopsis*, rice); the N-terminal extension of mature PSI-D specific to higher plants (II); and the C-terminal domain of PSI-D from higher plants that is highly similar to the corresponding segment of algal and cyanobacterial PSI-D proteins (III). Note that the N-terminal extension of the higher-plant proteins is rich in alanine and proline and highly diversified. The two mature *Arabidopsis* PSI-D proteins show amino acid exchanges at six positions of the N-terminal extension, but none in the C-terminal domain. Black boxes indicate strictly conserved amino acids, shaded boxes closely related amino acids. The symbol '+' refers to amino acid residues involved in the binding of ferredoxin (Bottin *et al.*, 2001; Hanley *et al.*, 1996; Lagoutte *et al.*, 2001); circles highlight lysine residues of the basic domain, which are important for the interaction of PSI-D with other PSI subunits (Chitnis *et al.*, 1997).

searched for insertions in the gene. A line was identified that carries a copy of the 5.2-kbp ROK2 T-DNA inserted 36 bp 5′ to the ATG of the *PsaD2* gene, and this mutant line was designated *psad2-1* (Figure 1b). A second *psad2* mutant allele was identified when DNA pools of the SALK collection of T-DNA lines were screened by PCR specific for insertions at the *PsaD2* locus. Out of the pool CS61661, the *psad2-2* line was isolated, which had a copy of the ROK2 T-DNA inserted 107 bp 5′ to the ATG of the *PsaD2* gene (Figure 1b).

Under greenhouse conditions, *psad1-1* plants were smaller than the wild type (WT) and had light-green leaves; in

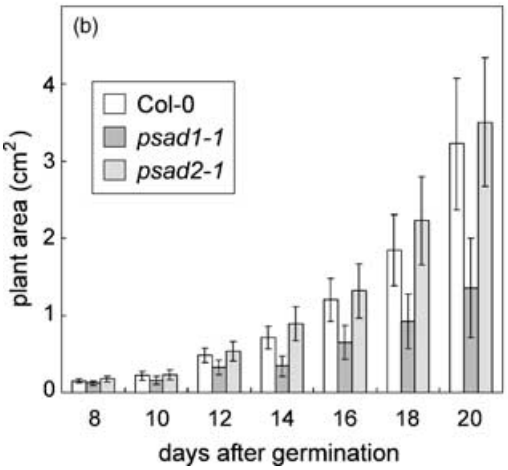

Figure 3. Phenotypes of *psad1-1*, *psad2-1*, *psad2-2* and the double mutant *psad1-1 psad2-1*.
(a) WT, *psad1-1*, *psad2-1* and *psad2-2* plants (4 weeks old) were grown in the greenhouse under long-day conditions.
(b) Growth kinetics of *psad1-1* and *psad2-1* mutants compared to WT. Thirty-six plants of each genotype were measured during the period from 8 to 20 days after germination. Mean values ± SDs (bars) are shown.
(c) WT and *psad1-1 psad2-1* double mutant plants (*d1 d2*) grown on sucrose-containing MS medium and illuminated with white light (top) or UV light (bottom).

contrast, both *psad2* lines showed WT-like growth and leaf coloration (Figure 3a). When the growth rates of the two single-gene mutants *psad1-1* and *psad2-1* were compared to that of WT plants (Leister *et al.*, 1999), growth of *psad1-1* plants was found to be substantially reduced compared to the mutants *psad2-1* and *psad2-2* (data not shown), and WT plants (Figure 3b). Crosses were carried out between *psad1-1* and *psad2-1*, and homozygous F_2 double-mutant plants were identified. The *psad1-1 psad2-1* double mutants did not survive when grown on soil, but could be propagated in axenic culture on medium supplemented with sucrose. Heterotrophically grown double mutants had yellowish leaves, remained very small and exhibited a high-chlorophyll-fluorescence (hcf) phenotype, similar to the mutant phenotypes previously observed by Meurer *et al.* (1996). This indicates that the absence of PSI-D causes a block in photosynthetic electron flow (Figure 3c). In addition, double mutants were highly photosensitive and could only be propagated under low-light conditions (photon flux density, PFD = 15 μmol photons m^{-2} sec^{-1}).

PsaD *expression*

Northern analysis revealed a marked decrease in the level of *PsaD* mRNA in *psad1-1*, and a slighter decrease in *psad2-1* (Figure 4a). Reverse-transcription PCR (RT-PCR) designed to discriminate between *PsaD1* and *PsaD2* transcripts indicated that in *psad1-1*, *PsaD1* transcript accumulation was completely suppressed, and that in *psad2-1* and *psad2-2*, the transcript of *PsaD2* was not detectable (Figure 4b). In the *psad1-1 psad2-1* double mutant, the accumulation of both forms of *PsaD* transcripts was completely suppressed (Figure 4c).

Western analyses demonstrated that the *psad1-1* mutant had 40% of WT amounts of PSI-D in thylakoids, while in *psad2-1* plants PSI-D was reduced by only 10% (Figure 5a; Table 1). In the double mutant *psad1-1 psad2-1*, no PSI-D was detected (Figure 5b; Table 1). Closer inspection of the D-specific immunoblot signals in the two single-gene mutants revealed that the gene products of *PsaD1* and *PsaD2* differed slightly in molecular mass, as one would expect from the predicted difference in the lengths of the mature proteins (PSI-D1, 164 amino acids; PSI-D2, 161 amino acids). In agreement with the transcription data, in *psad1-1*, only PSI-D2, and in *psad2-1*, only PSI-D1 were detectable. As residual PSI-D level in the two single-gene *psad* mutants added up to more than WT levels, it was concluded that – at least in *psad2-1* – the effects of the single-gene mutations were partially compensated by increased accumulation of the alternative PSI-D form.

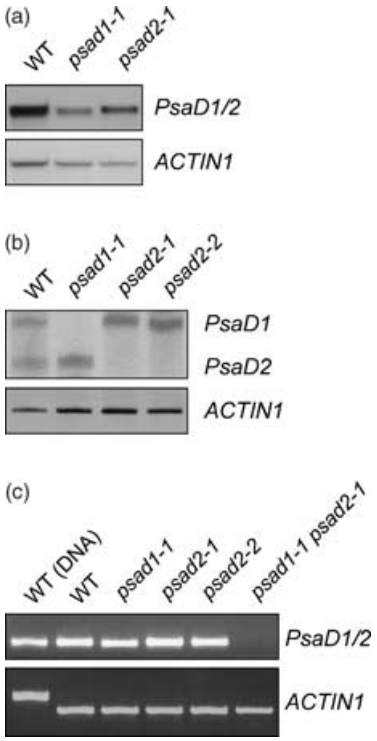

Figure 4. Expression of *PsaD* mRNA in mutant and WT plants.
(a) Northern analysis of *PsaD* transcripts. Aliquots (20 μg) of total RNA were hybridized with a mixture of *PsaD1* and *PsaD2* cDNA fragments. To control for variation in loading, the blots were probed with a cDNA fragment derived from the *ACTIN1* gene.
(b) Detection of *PsaD1* and *PsaD2* transcripts by RT-PCR. Products obtained after PCR for 35 cycles with *PsaD1*/*PsaD2* specific primers (PsaD1/2-22/22s and PsaD1/2-230/218as) and control primers for the *ACTIN1* gene in the same reactions were analysed on a 4.5% (w/v) polyacrylamide gel. The products derived from transcripts of the two *PsaD* genes differ in size by 12 bp and were visualized by silver staining.
(c) Detection of *PsaD* transcripts by RT-PCR. Products obtained after PCR for 35 cycles with primers recognizing both *PsaD* transcripts (PsaD1/2-22/22s and PsaD1/2-230/218as) and control primers for the *ACTIN1* gene were analysed on a 2.0% agarose gel. As a control, PCR with genomic WT-DNA was performed. The difference in size of the *ACTIN1* 'WT (DNA)' band is because of the presence of two introns in the genomic amplicon.

Increased dosage of the PsaD2 *gene can complement the* psad1-1 *mutation*

The almost identical sequence of the two mature PSI-D proteins suggested that PSI-D1 and -D2 have redundant functions. An experiment was carried out to complement the *psad1-1* mutation by introducing into the mutant background either the *PsaD1* or the *PsaD2* gene under transcriptional control of the 35S promoter. Increased dosage of either *PsaD1* or *PsaD2* in *psad1-1* could, in fact, restore the WT phenotype. In particular, the effect of the *psad1-1* mutation on effective quantum yield of PSII (WT, 0.76 ± 0.01; *psad1-1*, 0.52 ± 0.03; 35S::*PsaD1 psad1-1*, 0.76 ± 0.03; 35S::*PsaD2 psad1-1*, 0.77 ± 0.02), growth and leaf coloration could be fully reversed, demonstrating that *PsaD1* and *PsaD2* encode proteins with redundant functions. An explanation for the decrease of PSI-D in the *psad1-1* mutant is that the promoter of the *PsaD2* gene cannot drive sufficient expression of *PsaD2* to compensate the absence of *PsaD1* mRNA. In consequence, much less *PsaD* transcripts accumulate (see Figure 4a), and fewer PSI-D is synthesized (see Figure 5a).

PSI composition, accumulation of other thylakoid proteins and leaf pigments

The decrease in the amount of PSI-D in the *psad1-1* mutant was paralleled by a decrease in the levels of several PSI polypeptides, particularly of PSI-F, -H and -L, as well as of the four LHCI proteins (Figure 5a; Table 1). In the double mutant *psad1-1 psad2–1*, with the exception of traces of PSI-F, no accumulation of PSI core proteins was detectable. LHCI proteins were present but to a much lesser extent than in the WT (Figure 5b; Table 1), which is consistent with previous studies of barley (*Hordeum vulgare*) mutants that accumulate LHCI but no PSI core proteins (Hoyer-Hansen *et al.*, 1988; Nielsen *et al.*, 1996).

To reveal whether also the accumulation of other thylakoid proteins was affected, 2-D PAGE analyses were performed (Figure 6) and the intensity of signals was quantified (Table 1). In *psad1-1*, the level of PSI proteins was decreased, whereas PSII dimers accumulated to higher levels than in the WT ($PSII_D$ band in Figure 6a; spot 12 in Figure 6b). This accumulation was at the cost of monomeric forms (spots 2–4 in Figure 6b), suggesting that such dimeric forms are more stable in the mutant, possibly because of an altered pigment composition (see below). In *psad1-1 psad2-1* plants, no bands indicative for PSI complexes or for PSII dimers could be observed (Figure 6c,d), indicating a drastic reduction of PSII and pointing again to the absence of PSI complexes in this genotype.

Immunoblot analyses of proteins separated by denaturing 1-D PAGE (Figure 6e) revealed that in *psad1-1* thylakoids the accumulation of the Rieske protein, a subunit of the cyt b_6/f complex, was increased. The concentration of the α- and β-subunits of the ATPase complex appeared unchanged in *psad1-1* plants. This was in contrast to the results of 2-D PAGE analysis (Figure 6b), where a marked reduction of the α- and β-subunits of the chloroplast ATPase was detected. This discrepancy between the results of immunoblot analysis and 2-D gel analysis was reported before for another photosynthetic mutant (Varotto *et al.*, 2002b), and was interpreted as the result of a decreased stability of mutant ATPase during 2-D PAGE. In contrast to the *psad1-1* mutant, in the double mutant *psad1-1 psad2-1* the accumulation of the Rieske protein and of the ATPase (α- and β-subunits) was decreased (Figure 6e).

Effects of PSI-D mutations on leaf pigment composition were studied by HPLC (Table 2). WT levels of leaf

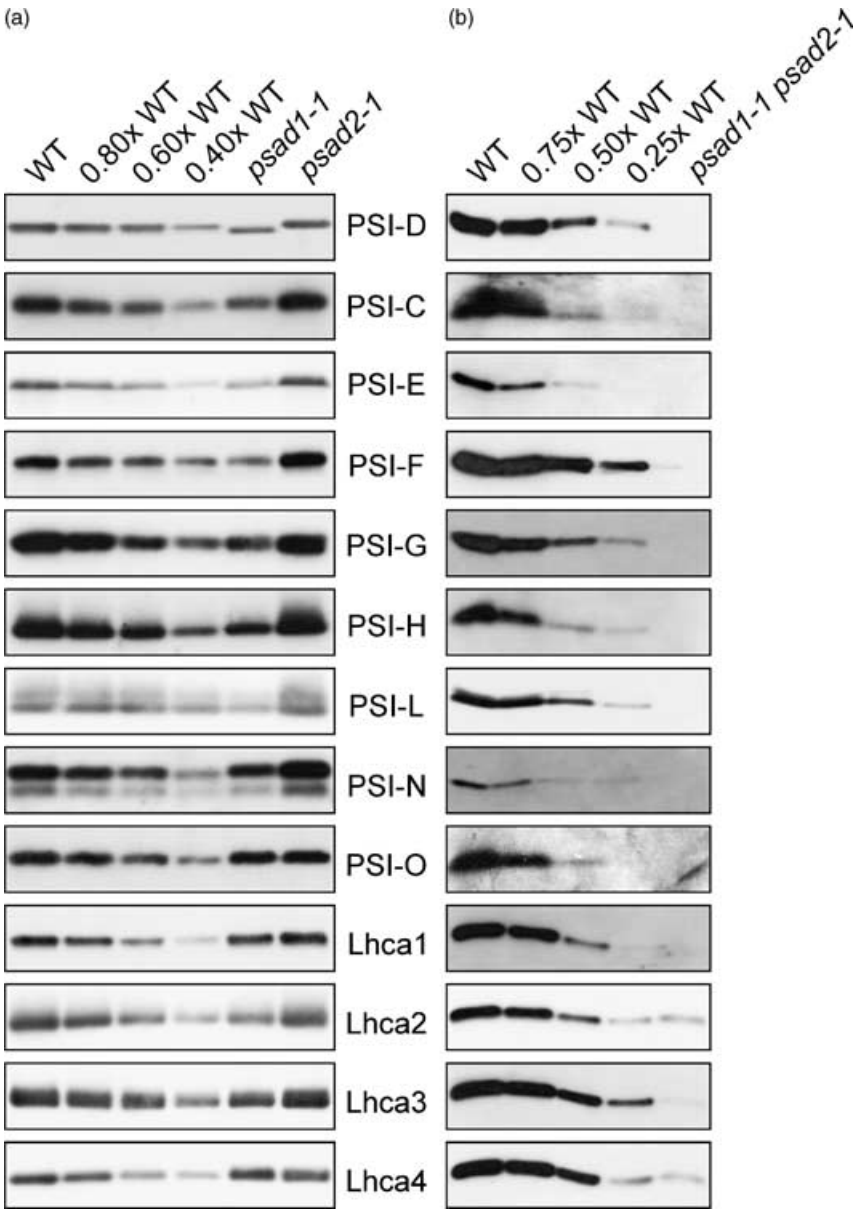

Figure 5. Levels of PSI polypeptides in mutant and WT plants.
Aliquots of thylakoid proteins corresponding to 5 μg of chlorophyll (*psad1-1*, *psad2-1* and WT plants; panel (a)), or 40 μg of total protein (*psad1-1 psad2-1* and WT plants; panel (b)) were loaded in each lane, and decreasing amounts of WT proteins were added to lanes 0.8×, 0.6× and 0.4× WT in panel (a), or to lanes 0.75×, 0.5× and 0.25× WT in panel (b). Replicate filters were immunolabelled with antibodies raised against individual PSI or LHCI polypeptides. Three independent experiments were performed, and representative results are shown. Signals obtained in three independent experiments were quantified using LUMI ANALYST 3.0 (Boehringer Mannheim/Roche). In the case of the *psad1-1* mutant, because of its reduced chlorophyll content, relatively more proteins were loaded. Relative values for the mutant genotypes, reflecting the ratio of expression between the mutant and WT (see Table 1), were normalized on the basis of their chlorophyll content (see Table 2). The PSI-D-specific immunoblot signals in *psad1-1* and *psad2-1* slightly differ in their molecular mass, as expected from the different predicted lengths of the mature proteins (PSI-D1, 164 amino acids; PSI-D2, 161 amino acids). When a mix of *psad1-1* and *psad2-1*, or of *psad1-1* and WT, or of *psad2-1* and WT thylakoid proteins was analysed, WT-like bands were detected (data not shown). This indicates that the two PSI-D forms can be discriminated only in the corresponding mutant backgrounds.

pigments were detected in the *psad2-1* mutant. In contrast, in *psad1-1* a disproportionate increase in the abundance of xanthophylls violaxanthin, antheraxanthin and zeaxanthin (VAZ) with respect to neoxanthin and lutein likely was observed. Chlorophyll content (Chl $a + b$) decreased by about 25% in *psad1-1*, which is consistent with the reduced amount of PSI and – to a less extent – of PSII complexes. The *psad1-1 psad2-1* double mutation resulted in a dramatic drop of chlorophyll (Chl $a + b$) and β-carotene content. Together with the lower chlorophyll *a*/*b* ratio, the data highlight a drastic reduction of PSII and, in particular, of PSI complexes. The relative increase of the VAZ pool size support an extreme photosensitivity of the double mutant.

Photosynthetic electron flow

Photosynthetic electron flow was characterized by measuring parameters of chlorophyll fluorescence and of $P700^+$ absorbance (Table 3). In *psad1-1* plants, the maximum quantum yield of PSII (F_V/F_M) was reduced when compared to *psad2-1* and WT plants. Moreover, the effective quantum yield of PSII (Φ_{II}) was substantially decreased in *psad1-1*, but not in *psad2-1* plants. Similarly, *psad2-1* showed normal photochemical (qP) and non-photochemical (qN) quenching. In contrast, in *psad1-1* the fraction of Q_A – the primary electron acceptor of PSII – present in the reduced state ($1 - qP$), was increased by about sixfold, indicating a partial block in the electron transfer steps

Table 1 Levels of PSI polypeptides in *psad1-1*, *psad2-1*, *psad1-1 psad2-1*, *psae1-1* and the antisense line Δ*F* relative to WT

PSI subunit	*psad1-1*	*psad2-1*	*psad1-1 psad2-1*	*psae1-1*	Δ*F*
A/B	nd	nd	nd	100	120
C	50	100	nd	30	60
D	40	90	0	30	40
E	40	100	0	30	40
F	20	100	2	100	40
G	40	90	0	100	nd
H	50	100	0	60	100
K	nd	nd	nd	nd	20
L	20	100	0	15	nd
N	50	100	0	100	50
O	70	100	0	nd	nd
Lhca1	70	100	1	100	100
Lhca2	50	100	30	100	100
Lhca3	50	100	5	100	100
Lhca4	70	100	20	100	120
Rieske	120	110	50	nd	nd
ATPase (α + β)	100	100	70	nd	nd
ATPase (α + β)*	20	nd	nd	nd	nd
PSII core*	70	nd	nd	nd	nd
OEC*	70	nd	nd	nd	nd
LHCII*	70	nd	nd	nd	nd
PSI*	40	nd	nd	nd	nd

psae1-1 and Δ*F* data are from Haldrup *et al.* (2000), Pesaresi *et al.* (2002, 2003b), and Varotto *et al.* (2000a). *psad1-1*, *psad2-1* and *psad1-1 psad2-1* signals from three independent experiments were quantified using LUMI ANALYST 3 (Boehringer Mannheim/Roche). Quantifications of proteins based on 2-D gel analysis are indicated by an asterisk (*). Relative values for the single mutant genotypes, reflecting the ratio of expression between the mutant and WT, were normalized on the basis of total chlorophyll content (see Table 2). Standard deviations were all within ±10%. Relative accumulation of proteins in the double mutant were not quantified after 2-D gel analysis (Figure 6d), because of non-linearity of silver staining. nd = data not determined.

downstream of Q_A. Also, qN slightly increased, supporting the conclusion that, as a consequence of the perturbation in photosynthetic electron flow, the thermal dissipation of excitation energy in the antenna of PSII was higher in *psad1-1* than in WT. Only negligible alterations in the reduction rate of P700 were found in the two single-gene mutants: $t_{1/2}$ox was not altered in *psad2-1*, but a pronounced delay in P700 oxidation was noted for *psad1-1*, suggesting an impairment of electron transfer from PSI to ferredoxin.

State transition quenching were followed by measuring maximum PSII fluorescence signals in states 1 (F_M1) and 2 (F_M2), after irradiating plants at wavelengths that target PSII and PSI, respectively, and normalizing the values to the maximum PSII fluorescence of dark-adapted leaves (F_M). In the WT, F_M1/F_M and F_M2/F_M differed significantly (0.84 ± 0.02 versus 0.75 ± 0.02), while in the *psad1-1* mutant, the two values were essentially the same (0.76 ± 0.02 versus 0.74 ± 0.02). This corresponds to a reduction of 70% in state transition quenching (qT) in the *psad1-1* mutant (Table 3), indicating a severe impairment in the re-distribution of excitation energy between the photosystems. In *psad2-1*, state transition quenching was similar to that in the WT (F_M1/F_M versus F_M2/F_M: 0.82 ± 0.02 versus 0.75 ± 0.01).

In *psad1-1 psad2-1* plants, photosynthetic electron flow was severely perturbed (Table 3). F_V/F_M was substantially decreased, as expected from a drastic reduction in the amount of active PSII centres. Moreover, the strong reduction in Φ_{II} was consistent with the high photosensitivity of the double mutant. The dramatically increased fraction of reduced Q_A (1 − qP) suggested that electron flow through PSII still occurred, while a block existed at a later electron transfer step. In general, *psad1-1 psad2-1* exhibited parameters of chlorophyll fluorescence induction similar to the ones of the plastocyanin-less mutant *pete1 pete2* (Weigel *et al.*, 2003) and the Rieske knock-out mutant *petc-2* (Maiwald *et al.*, 2003), both exhibiting a block in the linear electron flow.

In summary, only *psad1-1* seemed to be altered in photosynthetic electron flow. Interestingly, the chlorophyll fluorescence parameters of *psad1-1*, summarized above, were similar to those noted for *psae1-1* (Pesaresi *et al.*, 2002; Varotto *et al.*, 2000a), supporting the view that a reduction in the amount of either of these stromal proteins – which interact directly (Klukas *et al.*, 1999) – has similar effects on PSI function. Complete lack of PSI-D in *psad1-1 psad2-1* abolished photosynthetic electron flow and resulted in a dramatically increased photosensitivity.

Expression of mRNAs for nucleus-encoded chloroplast proteins in psad1-1

To test for further effects of the absence of PSI-D on photosynthesis and other chloroplast functions, the expression of nuclear genes contributing chloroplast functions was determined at the mRNA level by DNA array analysis. This was carried out for the *psad1-1* mutant, using a set of 3292 nuclear genes spotted on nylon membranes, 81% of which coding for chloroplast-targeted proteins, and the mRNA expression pattern observed was compared to that of the WT as described by Kurth *et al.* (2002), Pesaresi *et al.* (2003a) and Richly *et al.* (2003). Differential gene expression values (*psad1-1* versus WT) were determined by comparing hybridization signals. Among the 1101 genes that resulted differentially expressed, 574 were up- and 527 downregulated. The differentially expressed genes could be grouped into 13 major functional categories, including photosynthesis (dark or light reaction), metabolism, secondary metabolism, transcription, protein synthesis, protein phosphorylation, protein modification and fate, sensing, signalling and communication, stress response and transport (Figure 7). In general, genes for secondary metabolism, protein modification and fate, as well as for stress response,

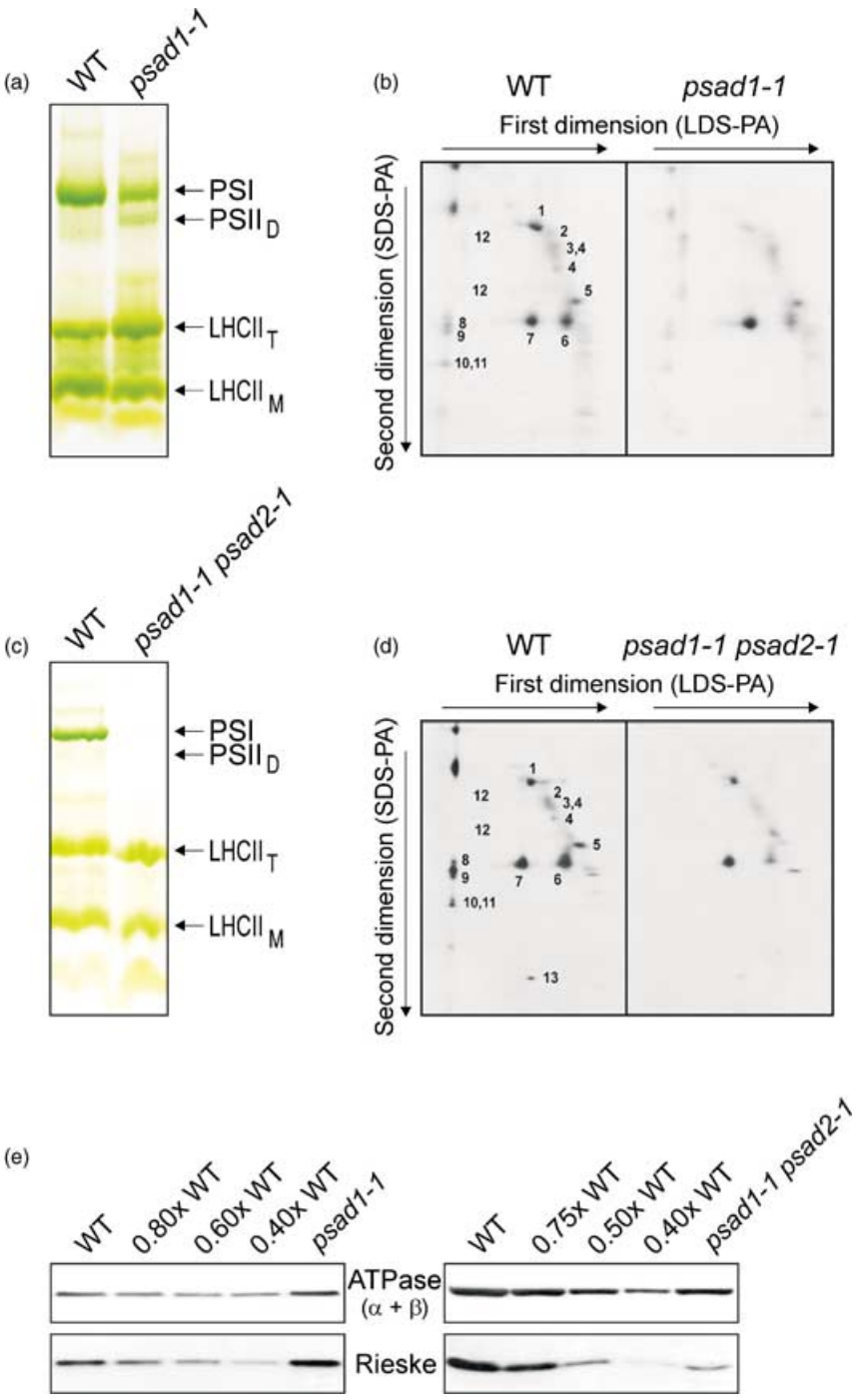

Figure 6. Protein composition of thylakoid membranes in mutant and WT plants.
(a, c) Thylakoid membranes corresponding to 30 μg of chlorophyll from WT and *psad1-1* (grown in the greenhouse) (a), or corresponding to 20 μg of chlorophyll from WT and *psad1-1 psad2-1* (grown in sterile culture) (c), were fractionated by electrophoresis on a LDS-PA gel. The bands were assigned to PSI, photosystem II dimers ($PSII_D$), LHCII trimers ($LHCII_T$) and monomers ($LHCII_M$).
(b, d) Thylakoid proteins separated by LDS–PAGE (see (a) and (c)) were fractionated on a denaturing SDS-PA gel. Positions of WT thylakoid proteins previously identified by Western analyses with appropriate antibodies are indicated by numbers to the right of the corresponding spots: 1, α- and β-subunits of the ATPase complex; 2, D1–D2; 3, CP47; 4, CP43; 5, oxygen-evolving complex (OEC); 6, LHCII monomer; 7, LHCII trimer; 8, PSI-D; 9, PSI-F; 10, PSI-C; 11, PSI-H; 12, PSII dimers; 13, cyt b_{559}. Considering the different leaf chlorophyll contents of the two genotypes, quantification (Table 1) was performed as described in the legend of Figure 5 and listed in Table 1. Relative accumulation of proteins in the double mutant was not quantified because of non-linearity of silver staining.
(e) Aliquots of thylakoid proteins corresponding to 5 μg of chlorophyll (*psad1-1* and WT plants; left panel), or 40 μg total protein (*psad1-1 psad2-1* and WT plants; right panel) were analysed as in Figure 5. Immunolabelling was performed with antibodies raised against the Rieske protein and the chloroplast ATPase (α- and β-subunits). Note that in the electrophoresis conditions used, the α- and β-subunits of the chloroplast ATPase could not be discriminated.

were upregulated more than others, supporting the conclusion that the impaired function of the thylakoid electron transport chain has profound effects on plant functions not directly related to photosynthesis. Preferentially, genes for the light reaction of photosynthesis and transcription were downregulated, implying that a response of the plant exists, aiming to limit and/or compensate the perturbation in photosynthetic electron flow by downregulating both chloroplast- and nucleus-encoded photosynthetic genes.

Discussion

Photosystem I subunit D is a hydrophilic subunit of PSI exposed on the stromal face and known to interact with ferredoxin in both eukaryotes and cyanobacteria (Andersen *et al.*, 1992; Merati and Zanetti, 1987; Zilber and Malkin, 1988). Together with PSI-C and -E, PSI-D forms a compact interconnected structure, the so-called stromal ridge (Jordan *et al.*, 2001; Klukas *et al.*, 1999; Kruip *et al.*,

Table 2 Pigment composition of leaves from *psad* mutants compared to WT

Leaf pigments	*psad1-1*	*psad2-1*	WT	*psad1-1 psad2-1**	WT*
Nx	36 ± 1	33 ± 1	33 ± 1	58 ± 1	40 ± 1
VAZ	80 ± 2	39 ± 0	36 ± 3	57 ± 3	24 ± 1
Lu	121 ± 2	116 ± 1	111 ± 2	239 ± 43	130 ± 1
β-Car	67 ± 1	76 ± 2	79 ± 3	25 ± 3	86 ± 1
Chl *a*/*b*	3.41 ± 0.03	3.46 ± 0.06	3.50 ± 0.06	2.38 ± 0.03	3.05 ± 0.02
Chl *a* + *b*	681 ± 121	883 ± 24	907 ± 115	223 ± 71	1797 ± 275

Pigment content was determined by HPLC of three plants for each genotype. The carotenoid content is given in mmol per mol Chl (*a* + *b*), and the Chl content is expressed as nmol Chl (*a* + *b*) per g FW. Mean values ± SD are shown. Nx, neoxanthin; VAZ, xanthophyll cycle pigments (violaxanthin + antheraxanthin + zeaxanthin); Lu, lutein; β-Car, β-carotene. The asterisk indicates genotypes grown on MS medium supplemented with sucrose.

Table 3 Spectroscopic data for mutant and WT leaves

Parameter	*psad1-1*	*psad2-1*	WT	*psad1-1 psad2-1**	WT*
F_v/F_m	0.77 ± 0.02	0.82 ± 0.01	0.83 ± 0.01	0.40 ± 0.07	0.80 ± 0.01
Φ_{II}	0.52 ± 0.03	0.75 ± 0.02	0.76 ± 0.01	0.07 ± 0.01	0.76 ± 0.01
1 − qP	0.30 ± 0.05	0.06 ± 0.02	0.05 ± 0.01	0.78 ± 0.03	0.03 ± 0.01
qN	0.23 ± 0.03	0.14 ± 0.01	0.17 ± 0.01	0.22 ± 0.08	0.05 ± 0.02
qT	0.03 ± 0.02	0.09 ± 0.03	0.12 ± 0.01	nd	nd
$t_{½}$red (msec)	63 ± 4	59 ± 2	57 ± 2	nd	nd
$t_{½}$ox (sec)	1.43 ± 0.16	0.54 ± 0.06	0.47 ± 0.06	nd	nd

Mean values for five plants (±SD) are shown. $t_{1/2}$red and $t_{1/2}$ox were calculated from the recorded kinetics of P700 reduction and re-oxidation. For greenhouse-grown plants, an actinic light intensity of 65 μmol photons m^{-2} sec^{-1} was used to drive electron transport before measuring. Because of its high photosensitivity, the double mutant and WT control plants were grown under low-light conditions (15 μmol photons m^{-2} sec^{-1}) on MS + sucrose (indicated by an asterisk (*)), and an actinic light intensity of 15 μmol photons m^{-2} sec^{-1} was applied to drive electron transport before measuring. nd: not determined.

1997). The characterization of *psad1-1* and *psad1-1 psad2-1* indicates that PSI-D is necessary for the stability of PSI in *Arabidopsis*, whereas *Synechocystis* PSI without PSI-D can still reduce flavodoxin (Xu *et al.*, 1994). In *Arabidopsis*, complete lack of the D subunit leads to seedling lethality under photoautotrophic conditions. The instability of *Arabidopsis* PSI without PSI-D can be explained either by degradation of the incomplete PSI complex or by down-regulation of the synthesis of PSI subunits.

In comparison to its cyanobacterial counterpart, the mature PSI-D from higher plants has an N-terminal extension of 20–30 amino acid residues. The N-terminal extension of PSI–D stabilizes the interaction of PSI-C with the rest of the PSI core (Naver *et al.*, 1995). Moreover, cross-linking experiments carried out in barley have suggested that PSI-D exerts its stabilizing effect via an interaction with PSI-H, an integral membrane protein located near PSI-I and PSI-L (Naver *et al.*, 1995). This suggestion is supported by the analysis of transgenic *Arabidopsis* lines co-suppressed for PSI-H, in which PSI-C is not as tightly bound to the PSI core as in the WT (Naver *et al.*, 1999). Our data are compatible with the hypothesis that PSI-D is in physical contact with PSI-H: in the *psad1-1* and *psad1-1 psad2-1* mutants, the decrease of PSI-D is, in fact, associated with a concomitant reduction in the level of PSI-H.

The changes of PSI polypeptide levels in *psad1-1* are reminiscent of those observed in the *psae1-1* mutant (Pesaresi *et al.*, 2002; Varotto *et al.*, 2000a) and in *PsaF* antisense plants (Δ*F*; Haldrup *et al.*, 2000; listed in Table 1). Considering that PSI-D and -E form, together with PSI-C, the stromal face of PSI, available results indicate that alterations in the expression of any of the peripheral stromal subunits de-stabilizes the entire stromal domain of PSI. In this context, it is not a surprise that the mRNA expression pattern of 3292 nuclear genes, most of them coding for chloroplast proteins, is very similar for the *psad1-1* and *psae1-1* mutants (Maiwald *et al.*, 2003). This supports the conclusion that a decreased accumulation of PSI-E or -D induce similar changes in the physiological state of the chloroplast. In this context, it is now clear that the coordinated partial loss of stromal polypeptides in the single-gene mutants *psae1-1* (Pesaresi *et al.*, 2002; Varotto *et al.*, 2000a), or *psad1-1* (this study), complicates the functional analysis of the role of individual stromal PSI polypeptides. As a starting point for future *in planta* studies of the function of the D- and E-subunits, double mutant lines like *psad1*

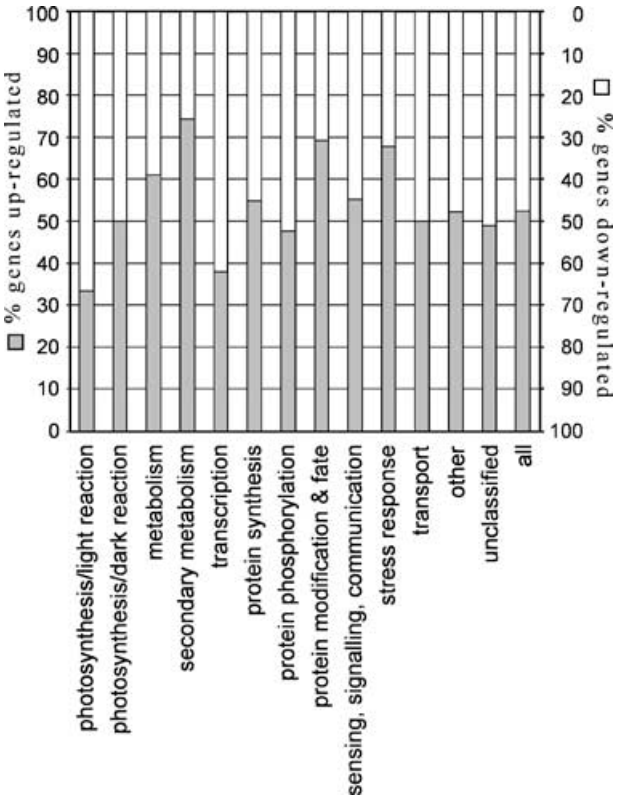

Figure 7. Effects of the *psad1-1* mutation on the accumulation of nuclear transcripts encoding chloroplasts proteins.
The fraction of up- and downregulated genes in 13 major functional categories is shown. A complete list of significantly differentially expressed genes is available at GEO (http://www.ncbi.nlm.nih.gov/geo/), Accession number GSM11018.

psad2 and *psae1 psae2* should be transformed with mutagenized functionally inactive versions of the concerned proteins, which retain the ability to stabilize the stromal domain of PSI.

Unlike the *psae1-1* mutant (Varotto *et al.*, 2000a), *psad1-1* plants show a reduction in the level of PSI-F and -N proteins (Table 1); a similar behaviour has been reported for ΔF lines (Haldrup *et al.*, 2000), supporting the observation that PSI-N co-varies with PSI-F (Pesaresi *et al.*, 2003b). PSI-H levels also decrease in *psad1-1* (this study) and in *psae1-1* (Pesaresi *et al.*, 2002) but not in ΔF lines (Haldrup *et al.*, 2000; Table 1), allowing to conclude that the effects of the absence of particular PSI polypeptides on the overall composition of PSI are not additive.

A marked decrease in the level of state transition quenching was noted in *psad1-1*. Whereas in *psae1-1*, a stable LHCII-PSI aggregate was responsible for the suppression of state transitions (Pesaresi *et al.*, 2002), no such aggregate exists in *psad1-1* (data not shown), pointing to a further difference in the consequences of the two mutations. Most likely, the suppression of state transitions in *psad1-1* is associated with the decrease in the abundance of PSI-H, the presumed docking site of LHCII (Lunde *et al.*, 2000).

The complementation of the *psad1-1* mutant by increased dosage of the *PsaD2* gene indicates that the two corresponding proteins are functionally redundant, and that the *psad1-1* phenotype is the result of a dosage effect of the two genes encoding the D subunit. The presence of two functional *Arabidopsis PsaD* genes raises the question of why these and other PSI genes are duplicated in the nuclear genome of *A. thaliana*. In *A. thaliana*, all of the gene pairs for PSI-E, -H and -D appear to have originated from relatively recent segmental duplications (between 24 and 40 million years ago; Blanc *et al.*, 2003), and the persistence of two functional genes for the same protein might have been under positive selection because it might have enabled responses of the same subunit to different signal transduction pathways. This would allow the plant cell to react more flexibly to environmental stimuli, as it seems to be the case for the PsaD gene family in *Nicotiana sylvestris*, where the *PsaD1* and *PsaD2* genes are differentially expressed during leaf development (Yamamoto *et al.*, 1993).

Experimental procedures

Plant lines, propagation and growth measurement

The screen for photosynthetic mutants was performed on 4-week-old, greenhouse-grown plants. Methods for propagation of *A. thaliana* plants under greenhouse conditions and for the measurement of their growth have been described by Leister *et al.* (1999).

The *psad1-1* mutant was identified among a collection of *dSpm*-mutagenized *A. thaliana* (ecotype Col-0) lines (SLAT collection; Tissier *et al.*, 1999) on the basis of a decrease in the effective quantum yield of PSII. The mutant *psad2-1* was identified in the SALK collection (http://signal.salk.edu/; Alonso *et al.*, 2003) which is made up of flank-tagged *ROK2* T-DNA lines (ecotype Col-0) by searching the insertion flanking database SIGNAL (http://signal.salk.edu/cgi-bin/tdnaexpress). The *psad2-2* mutant was identified in the SALK collection by PCR-screening hierarchically pooled plant DNA.

For the analysis of *psad1-1 psad2-2* double mutants, WT and double mutant plants were grown on Murashige and Skoog medium containing 2% Sucrose in a culture chamber on a 16-h-day period (PFD = 15 μmol photons m^{-2} sec^{-1}) at 22°C.

Analysis of nucleic acids

Arabidopsis DNA was isolated as described by Varotto *et al.* (2000a). Total leaf RNA was extracted using the RNeasy Plant System (Qiagen, Hilden, Germany). RNA gel blot analysis was performed under stringent conditions (Sambrook *et al.*, 1989) using a ^{32}P-labelled *PsaD1*/*PsaD2*-specific probe. Signals were quantified by using a phosphorimager (Storm 860; Molecular Dynamics, Sunnyvale, CA, USA) and the program IMAGE QUANT for MACINTOSH (version 1.2; Molecular Dynamics).

For RT-PCR analysis, first-strand cDNA was synthesized using the SuperScript Pre-amplification System (Invitrogen, Karlsruhe,

Germany). Products obtained after PCR for 35 cycles with *PsaD1*/*PsaD2*-specific primers and control primers for the *ACTIN1* gene in the same reactions were analysed on either 4.5% (w/v) polyacrylamide gel or 2% agarose gel. The products derived from transcripts of the two *PsaD* genes differ in size by 12 bp and were visualized by silver-stained polyacrylamide gel.

Sequence analysis

Sequence data were analysed with the Wisconsin Package Version 10.0, Genetics Computer Group, Madison, Wisconsin (GCG; Devereux *et al.*, 1984) and amino acid sequences were aligned using CLUSTALW (Thompson *et al.*, 1994). Chloroplast import sequence predictions were carried out using the TARGETP program (Emanuelsson *et al.*, 2000).

Complementation of the psad1-1 *mutant*

The *PsaD2* gene was ligated into the plant expression vector pJAN33 under the control of the Cauliflower Mosaic Virus 35S promoter. As a control 35S::*PsaD1* constructs were generated. Flowers of *psad1-1* mutant plants were transformed according to Clough and Bent (1998). Plants were transferred into the greenhouse, and seeds were collected after 3 weeks. Thirty-two independent transgenic plants for each 35S::*PsaD2* and 35S::*PsaD1* were selected on the basis of their resistance to kanamycin. Successful complementation was confirmed by measurements of chlorophyll fluorescence and growth. In addition, presence and overexpression of the transgene in the complemented mutant plants was confirmed by PCR and RT-PCR.

Chlorophyll fluorescence measurements

The procedure used to identify mutants that showed a change in Φ_{II}, the effective quantum yield of PSII ($\Phi_{II} = (F_M' - F_0')/F_M'$), has been described before by Varotto *et al.* (2000a,b). *In vivo* Chl *a* fluorescence of single leaves was measured using PAM 101/103 (Walz, Effeltrich, Germany) as described by Varotto *et al.* (2000a). To determine the maximum fluorescence (F_M) and the $(F_M - F_0)/F_M$ ratio ($=F_V/F_M$) 0.8-sec pulses of white light (6000 μmol photons m^{-2} sec^{-1}) were used. A 15-min illumination with actinic light (65 μmol photons m^{-2} sec^{-1} for single-gene mutants and WT grown on soil; 15 μmol photons m^{-2} sec^{-1} for double mutants and WT grown in sterile culture) was used to drive electron transport between PSII and PSI before measuring Φ_{II}, qN (non-photochemical quenching $= 1 - (F_M' - F_0')/(F_M - F_0)$), and qP (photochemical quenching $= (F_M' - F_S)/(F_M' - F_0)$).

State transitions were measured with a PAM 101/103 fluorometer (Walz, Effeltrich, Germany). After a 30-min incubation in the dark, the maximum fluorescence (F_M) of leaves was measured by using a saturating light pulse (0.8 sec, 6000 μmol photons m^{-2} sec^{-1}). Leaves were subsequently illuminated for 20 min with blue light (80 μmol photons m^{-2} sec^{-1}) from a Schott KL-1500 lamp equipped with a Walz BG39 filter. The maximum fluorescence in state 2 (F_M2), was then measured. Next, state 1 was induced by switching to far-red light (Walz 102-FR; peak emission 730 nm, 90 μmol photons m^{-2} sec^{-1}), and F_M1 was recorded 20 min later. qT was calculated according to the equation: $qT = (F_M1 - F_M2)/F_M2$ (Jensen *et al.*, 2000).

A dual-wavelength pulse-modulation system (ED-P700DW; Walz, Effeltrich, Germany) was used to record changes in the absorbance of $P700^+$. Leaves were illuminated with background far-red light, and immediately after full oxidation of P700, a saturating blue-light pulse (50 msec) was applied (XMT-103; Walz, Effeltrich, Germany) to reduce $P700^+$. $t_{1/2}$red and $t_{1/2}$ox were calculated from the recorded kinetics of P700 reduction and re-oxidation.

Western and 2-D PAGE analysis of proteins

Leaves from 4-week-old plants were harvested in the middle of the light period. Thylakoids were prepared as described by Bassi *et al.* (1985), and total proteins were isolated as described by Jensen *et al.* (2000). For 1-D PAGE analysis, protein amounts equivalent to 5 μg of chlorophyll (for *psad* single-gene mutants, see Figure 5a), or 40 μg of total proteins (for *psad1 psad2*, see Figure 5b) were loaded for each genotype. Decreasing amounts of WT proteins were loaded in parallel lanes (0.8× WT, 0.6× WT and 0.4× WT for *psad1-1* and *psad2-1*; 0.75× WT, 0.5× WT and 0.25× WT for *psad1-1 psad2-1*). For immunoblot analyses, proteins were transferred to Immobilon-P membranes (Millipore, Eschborn, Germany) and incubated with antibodies specific for individual polypeptides of PSI and LHCI. Signals were detected using the Enhanced Chemiluminescence Western Blotting Kit (Amersham Biosciences, Sunnyvale, CA, USA) and quantified using the LUMI ANALYST 3.0 (Boehringer Mannheim/Roche, Basel, Switzerland).

For 2-D gel analysis of WT and *psad1-1* plants, thylakoid membrane samples corresponding to 30 μg of chlorophyll were first fractionated on non-denaturing lithium dodecyl sulfate polyacrylamide (LDS-PA) gradient gels, and in the second dimension in a denaturing SDS-PA gradient (10–16%) gel, as described by Pesaresi *et al.* (2001, 2002). Proteins were visualized by Coomassie staining, and densitometric analyses of the protein gels were performed by using the LUMI ANALYST 3.0 (Boehringer Mannheim/Roche). Because of the limited amount of *psad1-1 psad2-1* samples, 2-D gel analysis was performed by using thylakoid membrane samples corresponding to 20 μg of chlorophyll. Proteins were visualized by silver staining.

Oligonucleotides (5′–3′ orientation) and isolation of insertion-flanking sequences

The regions flanking *dSpm* insertions were isolated by inverse PCR as described by Tissier *et al.* (1999). *PsaD1*- or *PsaD2*-specific sequences were amplified from WT and mutant plants using the primer pairs PsaD1-1s (ATGGCAACTCAAGCCGCCGG) and PsaD1-999as (TATGGTTTTGGATCGGAGACT) or PsaD2-226s (GTGGCATGTGGGAAACATATCC) and PsaD2-185as (CACGTAAAATTCCTCTACTTGTGCT); to amplify regions flanking the *dSpm* or *pROK2* insertions, the primer pairs dspm1 and dspm11 (Tissier *et al.*, 1999), LBa1 (http://signal.salk.edu/tdna_FAQs.html) and pROK2/pBIN19-460as (GTGCCCAGTCATAGCCGAATAGC) were used.

Primers that anneal to both *PsaD* genes were used for amplification of the *PsaD1*/*PsaD2*-specific Northern probe (PsaD1/2-22/22s, ATCTTCA(A/G)C(C/T)CCGCCATAACAACC; and PsaD1/2-441/429-as, CACTCTGTAAAACTGGTAAGTGATC); and for RT-PCR (PsaD1/2-22/22s and PsaD1/2-230/218as, GGTGTGTTTGGGTCTAGCTGCGG).

The *ACTIN1*-specific primers were ACTIN1-33s (TGCGACAATGGAACTGGAATG), ACTIN1-994as (GGATAGCATGTGGAAGTGCATACC).

Pigment analysis

Pigments were analysed by reversed-phase HPLC as described previously by Färber *et al.* (1997). For pigment extraction, leaf discs were frozen in liquid nitrogen and disrupted in a mortar in the

presence of acetone. After a short centrifugation, pigment extracts were filtered through a 0.2-μm membrane filter and either used directly for HPLC analysis or stored for up to 2 days at −20°C.

Expression profiling

The 3292-GST array, representing genes known or predicted to code for proteins featuring a chloroplast transit peptide (cTP), has been described previously by Richly *et al.* (2003). At least three experiments with different filters and independent cDNA probes derived from plant material corresponding to pools of at least 50 individuals were performed for each condition or genotype tested, thus minimizing variation between individual plants, filters or probes. cDNA probes were synthesized by using as primer a mixture of oligonucleotides matching the 3292 genes in antisense orientation, and hybridized to the GST array as described by Kurth *et al.* (2002) and Richly *et al.* (2003). Images were read using the Storm phosphorimager (Molecular Dynamics).

Hybridization images were imported into the ARRAYVISION program (version 6; Imaging Research Inc.), where artefacts were removed, background correction was performed and resulting values were normalized with reference to intensity of all spots on the array (Kurth *et al.*, 2002; Richly *et al.*, 2003). In the next step, those data were imported into the ARRAYSTAT program (version 1.0 Rev. 2.0; Imaging Research Inc.) and a *z*-test (nominal α set to 0.05) was performed to identify statistically significant differential expression values as described by Pesaresi *et al.* (2003a). Only differential expression values fulfilling the criteria of the *z*-test are listed in the Supplementary Material.

Accession of mRNA expression profiling data

Primary data of the mRNA profile of the *psad1-1* mutant are available at the Gene Expression Omnibus (GEO) site (http://www.ncbi.nlm.nih.gov/geo/), Accession number GSM11018.

Acknowledgements

We thank the Salk Institute Genomic Analysis Laboratory for providing the sequence-indexed *Arabidopsis* T-DNA insertion mutants, as well as the Sainsbury Laboratory for making *dSpm*-tagged lines publicly available. Grateful acknowledgements are extended to Paul Hardy for critical reading of the manuscript. This work was supported by the European Community's Human Potential Programme (contract no. HPRN-CT-2002-00248 (PSI-CO)), and by the Deutsche Forschungsgemeinschaft (DL 1265-1 and -8, and III GK – GRK 306/1).

Supplementary Material

The following material is available from http://www.blackwellpublishing.com/products/journals/suppmat/TPJ/TPJ2011/TPJ2011sm.htm

Table S1 List of significantly differentially expressed genes in *psad1-1* (compared to the WT) and their classification

References

Alonso, J.M., Stepanova, A.N., Leisse, T.J. *et al.* (2003) Genome-wide insertional mutagenesis of *Arabidopsis thaliana*. *Science*, **301**, 653–657.

Andersen, B., Koch, B. and Scheller, H.V. (1992) Structural and functional analysis of the reducing side of photosystem I. *Physiol. Plant.* **84**, 154–161.

Bassi, R., dal Belin Peruffo, A., Barbato, R. and Ghisi, R. (1985) Differences in chlorophyll-protein complexes and composition of polypeptides between thylakoids from bundle sheaths and mesophyll cells in maize. *Eur. J. Biochem.* **146**, 589–595.

Blanc, G., Hokamp, K. and Wolfe, K.H. (2003) A recent polyploidy superimposed on older large-scale duplications in the *Arabidopsis* genome. *Genome Res.* **13**, 137–144.

Bottin, H., Hanley, J. and Lagoutte, B. (2001) Role of acidic amino acid residues of PsaD subunit on limiting the affinity of photosystem I for ferredoxin. *Biochem. Biophys. Res. Commun.* **287**, 833–836.

Chitnis, V.P. and Chitnis, P.R. (1993) PsaL subunit is required for the formation of photosystem I trimers in the cyanobacterium *Synechocystis* sp. PCC 6803. *FEBS Lett.* **336**, 330–334.

Chitnis, P.R., Reilly, P.A. and Nelson, N. (1989) Insertional inactivation of the gene encoding subunit II of photosystem I from the cyanobacterium *Synechocystis* sp. PCC 6803. *J. Biol. Chem.* **264**, 18381–18385.

Chitnis, V.P., Ke, A. and Chitnis, P.R. (1997) The PsaD subunit of photosystem I. Mutations in the basic domain reduce the level of PsaD in the membranes. *Plant Physiol.* **115**, 1699–1705.

Clough, S.J. and Bent, A.F. (1998) Floral dip: a simplified method for *Agrobacterium*-mediated transformation of *Arabidopsis thaliana*. *Plant J.* **16**, 735–743.

Devereux, J., Haeberli, P. and Smithies, O. (1984) A comprehensive set of sequence analysis programs for the VAX. *Nucl. Acids Res.* **12**, 387–395.

Emanuelsson, O., Nielsen, H., Brunak, S. and von Heijne, G. (2000) Predicting subcellular localization of proteins based on their N-terminal amino acid sequence. *J. Mol. Biol.* **300**, 1005–1016.

Färber, A., Young, A.J., Ruban, A.V., Horton, P. and Jahns, P. (1997) Dynamics of xanthophyll-cycle activity in different antenna subcomplexes in the photosynthetic membranes of higher plants: the relationship between zeaxanthin conversion and nonphotochemical fluorescence quenching. *Plant Physiol.* **115**, 1609–1618.

Haldrup, A., Naver, H. and Scheller, H.V. (1999) The interaction between plastocyanin and photosystem I is inefficient in transgenic *Arabidopsis* plants lacking the PSI-N subunit of photosystem I. *Plant J.* **17**, 689–698.

Haldrup, A., Simpson, D.J. and Scheller, H.V. (2000) Down-regulation of the PSI-F subunit of photosystem I (PSI) in *Arabidopsis thaliana*. The PSI-F subunit is essential for photoautotrophic growth and contributes to antenna function. *J. Biol. Chem.* **275**, 31211–31218.

Haldrup, A., Lunde, C. and Scheller, H.V. (2003) Plants lacking the PSI-D subunit of photosystem I suffer severe photoinhibition, have unstable photosystem I complexes and altered redox homeostasis in the chloroplast stroma. *J. Biol. Chem.* **278**, 33276–33283.

Hanley, J., Setif, P., Bottin, H. and Lagoutte, B. (1996) Mutagenesis of photosystem I in the region of the ferredoxin cross-linking site: modifications of positively charged amino acids. *Biochemistry*, **35**, 8563–8571.

Hoyer-Hansen, G., Bassi, R., Honberg, L.S. and Simpson, D.J. (1988) Immunological characterization of chlorophyll *a*/*b*-binding proteins of barley thylakoids. *Planta*, **173**, 12–21.

Jansson, S. (1999) A guide to the Lhc genes and their relatives in *Arabidopsis*. *Trends Plant Sci.* **4**, 236–240.

Jensen, P.E., Gilpin, M., Knoetzel, J. and Scheller, H.V. (2000) The PSI-K subunit of photosystem I is involved in the interaction

between light-harvesting complex I and the photosystem I reaction center core. *J. Biol. Chem.* **275**, 24701–24708.

Jensen, P.E., Rosgaard, L., Knoetzel, J. and Scheller, H.V. (2002) Photosystem I activity is increased in the absence of the PSI-G subunit. *J. Biol. Chem.* **277**, 2798–2803.

Jordan, P., Fromme, P., Witt, H.T., Klukas, O., Saenger, W. and Krauss, N. (2001) Three-dimensional structure of cyanobacterial photosystem I at 2.5 Å resolution. *Nature*, **411**, 909–917.

Kitmitto, A., Holzenburg, A. and Ford, R.C. (1997) Two-dimensional crystals of photosystem I in higher plant grana margins. *J. Biol. Chem.* **272**, 19497–19501.

Klukas, O., Schubert, W.D., Jordan, P., Krauss, N., Fromme, P., Witt, H.T. and Saenger, W. (1999) Photosystem I, an improved model of the stromal subunits PsaC, PsaD, and PsaE. *J. Biol. Chem.* **274**, 7351–7360.

Knoetzel, J., Mant, A., Haldrup, A., Jensen, P.E. and Scheller, H.V. (2002) PSI-O, a new 10-kDa subunit of eukaryotic photosystem I. *FEBS Lett.* **510**, 145–148.

Kruip, J., Chitnis, P.R., Lagoutte, B., Rogner, M. and Boekema, E.J. (1997) Structural organization of the major subunits in cyanobacterial photosystem I. Localization of subunits PsaC, -D, -E, -F, and -J. *J. Biol. Chem.* **272**, 17061–17069.

Kurth, J., Varotto, C., Pesaresi, P., Biehl, A., Richly, E., Salamini, F. and Leister, D. (2002) Gene-sequence-tag expression analyses of 1,800 genes related to chloroplast functions. *Planta*, **215**, 101–109.

Lagoutte, B., Hanley, J. and Bottin, H. (2001) Multiple functions for the C terminus of the PsaD subunit in the cyanobacterial photosystem I complex. *Plant Physiol.* **126**, 307–316.

Leister, D., Varotto, C., Pesaresi, P., Niwergall, A. and Salamini, F. (1999) Large-scale evaluation of plant growth in *Arabidopsis thaliana* by non-invasive image analysis. *Plant Physiol. Biochem.* **37**, 671–678.

Lunde, C., Jensen, P.E., Haldrup, A., Knoetzel, J. and Scheller, H.V. (2000) The PSI-H subunit of photosystem I is essential for state transitions in plant photosynthesis. *Nature*, **408**, 613–615.

Maiwald, D., Dietzmann, A., Jahns, P., Pesaresi, P., Joliot, P., Joliot, A., Levin, J.Z., Salamini, F. and Leister, D. (2003) Knock-out of the genes coding for the Rieske protein and the ATP-synthase δ-subunit of *Arabidopsis thaliana*. Effects on photosynthesis, thylakoid protein composition and nuclear chloroplast gene expression. *Plant Physiol.* **133**, 191–202.

Mannan, R.M., Pakrasi, H.B. and Sonoike, K. (1994) The PsaC protein is necessary for the stable association of the PsaD, PsaE, and PsaL proteins in the photosystem I complex: analysis of a cyanobacterial mutant strain. *Arch. Biochem. Biophys.* **315**, 68–73.

Merati, G. and Zanetti, G. (1987) Chemical cross-linking of ferredoxin to spinach thylakoids – evidence for two independent binding-sites of ferredoxin to the membrane. *FEBS Lett.* **215**, 37–40.

Meurer, J., Meierhoff, K. and Westhoff, P. (1996) Isolation of high-chlorophyll fluorescence mutants of *Arabidopsis thaliana* and their characterization by spectroscopy, immunoblotting and Northern hybridization. *Planta*, **198**, 385–396.

Naver, H., Scott, M.P., Andersen, B., Moller, B.L. and Scheller, H.V. (1995) Reconstitution of barley photosystem I reveals that the N-terminus of the PSI-D subunit is essential for tight binding of PSI-C. *Physiol. Plant.* **95**, 19–26.

Naver, H., Haldrup, A. and Scheller, H.V. (1999) Cosuppression of photosystem I subunit PSI-H in *Arabidopsis thaliana*. Efficient electron transfer and stability of photosystem I is dependent upon the PSI-H subunit. *J. Biol. Chem.* **274**, 10784–10789.

Nielsen, V.S., Scheller, H.V. and Moller, B.L. (1996) The photosystem I mutant *viridis-zb*^{63} of barley (*Hordeum vulgare*) contains low amounts of active but unstable photosystem I. *Physiol. Plant.* **98**, 637–644.

Pesaresi, P., Varotto, C., Meurer, J., Jahns, P., Salamini, F. and Leister, D. (2001) Knock-out of the plastid ribosomal protein L11 in *Arabidopsis*: effects on mRNA translation and photosynthesis. *Plant J.* **27**, 179–189.

Pesaresi, P., Lunde, C., Jahns, P. *et al.* (2002) A stable LHCII-PSI aggregate and suppression of photosynthetic state transitions in the *psae1-1* mutant of *Arabidopsis thaliana*. *Planta*, **215**, 940–948.

Pesaresi, P., Gardner, N.A., Masiero, S., Dietzmann, A., Eichacker, L., Wickner, R., Salamini, F. and Leister, D. (2003a) Cytoplasmic N-terminal protein acetylation is required for efficient photosynthesis in *Arabidopsis*. *Plant Cell*, **15**, 1817–1832.

Pesaresi, P., Varotto, C., Richly, E., Leßnick, A., Salamini, F. and Leister, D. (2003b) Protein-protein and protein-function relationships in *Arabidopsis* photosystem I: cluster analysis of PSI polypeptide levels and photosynthetic parameters in PSI mutants. *J. Plant Physiol.* **160**, 17–22.

Richly, E., Dietzmann, A., Biehl, A., Kurth, J., Laloi, C., Apel, K., Salamini, F. and Leister, D. (2003) Co-variations in the nuclear chloroplast transcriptome reveal a regulatory master switch. *EMBO Rep.* **4**, 491–498.

Sambrook, J., Fritsch, E.F. and Maniatis, T. (1989) *Molecular Cloning: a Laboratory Manual*, 2nd edn. Cold Spring Harbor: Cold Spring Harbor Laboratory Press.

Scheller, H.V., Jensen, P.E., Haldrup, A., Lunde, C. and Knoetzel, J. (2001) Role of subunits in eukaryotic photosystem I. *Biochim. Biophys. Acta*, **1507**, 41–60.

Thompson, J.D., Higgins, D.G. and Gibson, T.J. (1994) CLUSTAL W: improving the sensitivity of progressive multiple sequence alignment through sequence weighting, position-specific gap penalties and weight matrix choice. *Nucl. Acids Res.* **22**, 4673–4680.

Tissier, A.F., Marillonnet, S., Klimyuk, V., Patel, K., Torres, M.A., Murphy, G. and Jones, J.D. (1999) Multiple independent defective *Suppressor-mutator* transposon insertions in *Arabidopsis*: a tool for functional genomics. *Plant Cell*, **11**, 1841–1852.

Varotto, C., Pesaresi, P., Meurer, J., Oelmuller, R., Steiner-Lange, S., Salamini, F. and Leister, D. (2000a) Disruption of the *Arabidopsis* photosystem I gene *psaE1* affects photosynthesis and impairs growth. *Plant J.* **22**, 115–124.

Varotto, C., Pesaresi, P., Maiwald, D., Kurth, J., Salamini, F. and Leister, D. (2000b) Identification of photosynthetic mutants of *Arabidopsis* by automatic screening for altered effective quantum yield of photosystem 2. *Photosynthetica*, **38**, 497–504.

Varotto, C., Pesaresi, P., Jahns, P., Leßnick, A., Tizzano, M., Schiavon, F., Salamini, F. and Leister, D. (2002a) Single and double knock-outs of the genes for photosystem I subunits PSI-G, -K and -H of *Arabidopsis thaliana*: effects on PSI composition, photosynthetic electron flow and state transitions. *Plant Physiol.* **129**, 616–624.

Varotto, C., Maiwald, D., Pesaresi, P., Jahns, P., Salamini, F. and Leister, D. (2002b) The metal ion transporter IRT1 is necessary for iron homeostasis and efficient photosynthesis in *Arabidopsis thaliana*. *Plant J.* **31**, 589–599.

Weigel, M., Varotto, C., Pesaresi, P., Finazzi, G., Rappaport, F., Salamini, F. and Leister, D. (2003) Plastocyanin is indispensable for photosynthetic electron flow in *Arabidopsis thaliana*. *J. Biol. Chem.* **278**, 31286–31289.

Xu, Q., Jung, Y.S., Chitnis, V.P., Guikema, J.A., Golbeck, J.H. and Chitnis, P.R. (1994) Mutational analysis of photosystem I

polypeptides in *Synechocystis* sp. PCC 6803. Subunit requirements for reduction of $NADP^+$ mediated by ferredoxin and flavodoxin. *J. Biol. Chem.* **269**, 21512–21518.

Yamamoto, Y., Tsuji, H. and Obokata, J. (1993) Structure and expression of a nuclear gene for the PSI-D subunit of photosystem I in *Nicotiana sylvestris*. *Plant Mol. Biol.* **22**, 985–994.

Yu, J., Smart, L.B., Jung, Y.S., Golbeck, J. and McIntosh, L. (1995) Absence of PsaC subunit allows assembly of photosystem I core but prevents the binding of PsaD and PsaE in *Synechocystis* sp. PCC6803. *Plant Mol. Biol.* **29**, 331–342.

Zhao, J., Snyder, W.B., Mühlenhoff, U., Rhiel, E., Warren, P.V., Golbeck, J.H. and Bryant, D.A. (1993) Cloning and characterization of the *psaE* gene of the cyanobacterium *Synechococcus* sp. PCC 7002: characterization of a *psaE* mutant and overproduction of the protein in *Escherichia coli*. *Mol. Microbiol.* **9**, 183–194.

Zilber, A.L. and Malkin, R. (1988) Ferredoxin cross-links to a 22-kD subunit of photosystem I. *Plant Physiol.* **88**, 810–814.